ACS APPLIED MATERIALS & INTERFACES

Letter

www.acsami.org

Functionalized Graphene as an Ultrathin Seed Layer for the Atomic Layer Deposition of Conformal High-*k* Dielectrics on Graphene

Woo Cheol Shin, Jae Hoon Bong, Sung-Yool Choi, and Byung Jin Cho*

Department of Electrical Engineering, KAIST, Daejeon, Korea 305-701

ABSTRACT: Ultrathin functionalized graphene (FG) is demonstrated to work as an effective seed layer for the atomic layer deposition (ALD) of high-k dielectrics on graphene that is synthesized via chemical vapor deposition (CVD). The FG layer is prepared using a low-density oxygen plasma treatment on CVD graphene and is characterized using Raman spectroscopy and X-ray photoelectron spectroscopy (XPS). While the ALD deposition on graphene results in a patchy and rough dielectric deposition, the abundant oxygen species provided by the FG seed layer enable conformal and pinhole-free dielectric film deposition over the entire area of the graphene channel. The metal-insulator-graphene (MIG) capacitors fabricated with the FG-seeded Al_2O_3 exhibit superior scaling capabilities with low leakage currents when compared with the co-processed capacitors with Al seed layers.

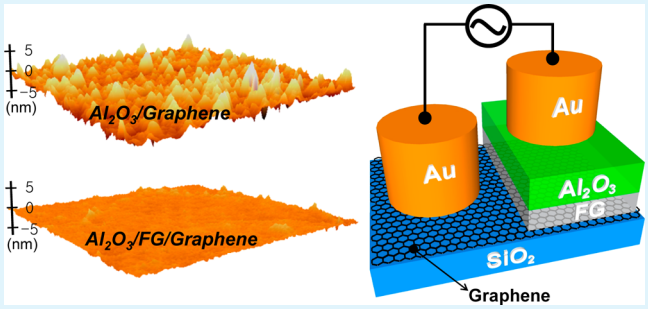

KEYWORDS: *CVD graphene, functionalized graphene, ALD, dielectrics, capacitors*

INTRODUCTION

Graphene has emerged as a promising active layer that enables high speed transistors due to its outstanding intrinsic mobility, high saturation velocity, and two-dimensional (2D) planar structure.[1,2] Based on these superb characteristics, graphene radio frequency (RF) transistors have been investigated extensively in an effort to improve their electrical performance in terms of field effect mobility, transconductance, current saturation, and cut-off frequency.[3−6] To achieve high-performance graphene devices, the integration of gate dielectrics into graphene channels has been considered as a significant process because the formation of ultrathin, high quality dielectrics on graphene is a prerequisite for reduced extrinsic scattering at the graphene-dielectric interface, low operating voltage, scaling capability, and device reliability. Atomic layer deposition (ALD) is an ideal technique for depositing ultrathin dielectric films because it enables precise thickness control and excellent uniformity.[7] However, the ALD of conformal dielectric films on graphene is difficult due to the chemical inertness of the graphene surface and its hydrophobicity.[8,9] As a result, various approaches have been adopted prior to the gate dielectric deposition on graphene, including the use of metal seed layers,[10−12] polymer coatings,[13−15] and plasma-assisted functionalization.[16,17] However, these approaches using naturally oxidized metals or polymer spin-coating increases the difficulty of controlling the film thickness, thus presenting limitations in scaling the gate dielectric thickness. This is a significant drawback given that high gate capacitance is critical for realizing the low voltage operation of graphene devices. In this respect, the plasma-assisted functionalization is a more promising technique considering that it directly functionalizes the graphene surface without introducing additional seed layers. However, it is well-known that direct exposure to oxygen plasma causes ion bombardment damage, which ultimately leads to large amounts of disorders in the graphene.[18,19]

In this work, a new approach to facilitating the ALD of high-k dielectrics on chemical vapor deposition (CVD) graphene is proposed using an additional functionalized graphene (FG) monolayer as an ultrathin seed layer on top of the graphene channel. A large-scale FG layer was prepared using a low-power oxygen plasma treatment on CVD graphene and was characterized using Raman spectroscopy and X-ray photoelectron spectroscopy (XPS). The resulting FG layer was transferred onto a graphene channel on an oxidized silicon wafer, which resulted in the formation of an ultrathin seed layer on the graphene. This graphene functionalization process based on the additional FG layer is highly desirable in terms of preserving the lattice of the graphene channel, given that the underlying graphene is indirectly functionalized using another CVD graphene sheet. The subsequent ALD on the FG/graphene/SiO_2 led to continuous and conformal Al_2O_3 on the graphene with a surface roughness of ∼0.3 nm. Finally, the metal-insulator-graphene (MIG) capacitors consisting of Au/Al_2O_3/FG/graphene and Au/Al_2O_3/oxidized Al/graphene were fabricated and characterized in order to assess their insulating properties. The FG-seeded Al_2O_3 dielectric exhibited a low leakage current density of 7×10^{-9} A/cm^2 at 3 MV/cm. Furthermore, the use of the FG seed layer enabled a lower equivalent oxide thickness (EOT) compared with that of the Al

Received: September 13, 2013
Accepted: October 30, 2013
Published: October 30, 2013

metal seed layer, and this was attributed to the ultrathin thickness of the FG layer.

EXPERIMENTAL SECTION

Figure 1 describes the processing steps required for the preparation of the functionalized graphene (FG) and its

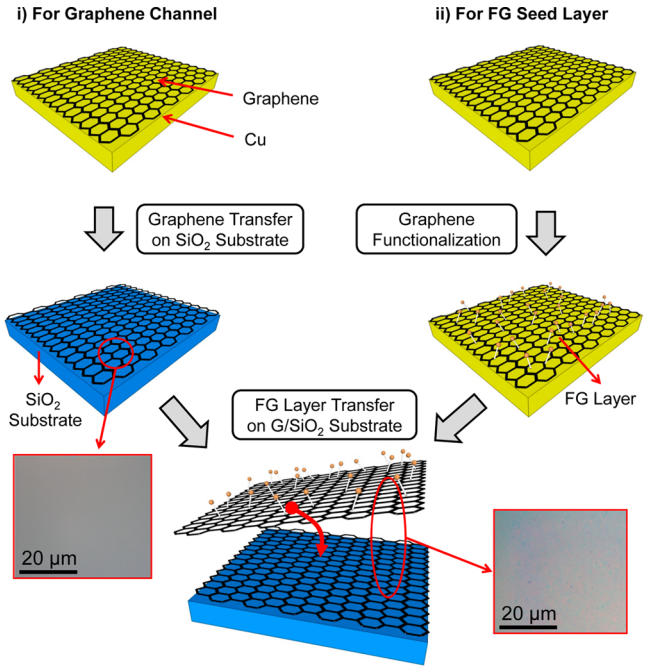

Figure 1. Schematic diagram of the fabrication process for the FG seed layer formation on graphene. The FG seed layer prepared using a low-density oxygen plasma treatment on CVD graphene grown on Cu was subsequently transferred to graphene/SiO_2 substrates using a wet transfer process. The graphene channel was indirectly functionalized using another CVD graphene sheet.

application to the seed layer on graphene. The monolayer graphene was synthesized using a CVD process based on inductively coupled plasma (ICP) on a Cu/SiO_2/Si substrate. The sample was heated in ambient Ar and then exposed to H_2 plasma with a gas flow rate of 40 sccm and an RF plasma power of 50 W for 2 min. A mixture of Ar and C_2H_2 was flowed into the ICP CVD chamber to assist the graphene growth process. For the FG layer preparation, the as-grown graphene on the Cu was exposed to low-density oxygen plasma that was obtained through sustaining plasma with 40 W. A pressure of 200 mTorr and an O_2 flow of 50 sccm were used. To form the ultrathin seed layer on graphene, we transferred the FG layer to a graphene/SiO_2 substrate using the conventional wet transfer process with poly(methyl methacrylate) (PMMA) supporting layer. After the transfer of the PMMA/FG layer, the PMMA/FG/graphene/SiO_2 substrate was annealed at 350 °C in ambient H_2 in order to remove the PMMA residue from the FG layer. It was observed that the removal of PMMA using the H_2 annealing is effective to reduce the PMMA residues on FG surface. Then, the Al_2O_3 film was deposited on top of the FG/graphene/SiO_2 and graphene/SiO_2 substrates using 200 cycles of ALD. The ALD of Al_2O_3 was performed using trimethyl aluminum (TMA; 99.99%, Aldrich,) and H_2O as a precursor and oxygen source, respectively. The film thicknesses were confirmed through measuring the edge height of the film using atomic force microscopy (AFM).[20] The MIG capacitors (Au/dielectrics/graphene) were fabricated separately in order to evaluate the dielectric properties. Au dots with a thickness of 100 nm and a diameter of 200 μm were thermally evaporated onto the Al_2O_3 dielectric film in order to form the top electrodes. The electrical measurements for the MIG capacitors were performed in ambient air.

RESULTS AND DISCUSSION

The FG layer was prepared using a low-density plasma treatment on CVD graphene. Figure 2 shows the Raman

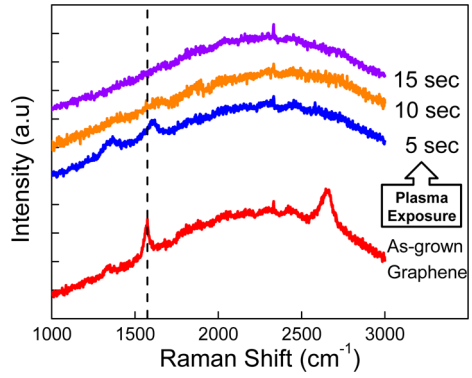

Figure 2. Raman spectra for the CVD graphene exposed to the oxygen plasma for different exposure time periods. The CVD graphene was exposed to low-density plasma (40 W) for 5 s in order to functionalize the graphene. The variation in the D and 2D bands following the functionalization exhibited additional defects that were generated by the attachment of oxygen-terminated groups in the FG layer. In addition, the G-band broadened and exhibited a shift to a higher frequency.

spectra for the CVD graphene exposed to the oxygen plasma for different exposure time periods. The plasma treatment condition was adjusted to be low power plasma (40 W) in order to functionalize the graphene while avoiding complete etching of the graphene. For plasma exposure times greater than 10 s, graphene peaks were not found in the Raman spectra, which indicate that the graphene is gradually etched within 10 s. For the graphene functionalization, the CVD graphene was exposed to plasma for 5 s. As a result, significant changes were observed in the graphene Raman peaks. The D-band became more prominent and this was attributed to the structural defects generated by the attachment of oxygen-terminated functional groups to the graphene plane. The absence of a 2D band indicates the lack of an sp^2 carbon network in the FG. Furthermore, the G-band broadened significantly and exhibited a shift to a higher frequency (blue shift). This behavior of the Raman features for the FG layer is similar to previous studies on the functionalization of graphites and graphene oxides.[21,22]

The FG was used as a seed layer in order to facilitate the ALD of high-k dielectrics on the graphene surface. The sample with the direct ALD of high-*k* dielectrics on the graphene was also prepared for comparison. Prior to the ALD process, the graphene grown on the Cu film was transferred to the SiO_2 substrate via a conventional wet transfer process.[13] The 20 nm-thick Al_2O_3 film was then deposited on the graphene/SiO_2 substrate. Figure 3(b) presents the AFM images of the surface of Al_2O_3 deposited on the graphene and FG/graphene. Unlike mechanically exfoliated graphene flakes[23] and highly oriented pyrolytic graphite (HOPG),[17] the CVD graphene was

dx.doi.org/10.1021/am4039807 | ACS Appl. Mater. Interfaces 2013, 5, 11515−11519

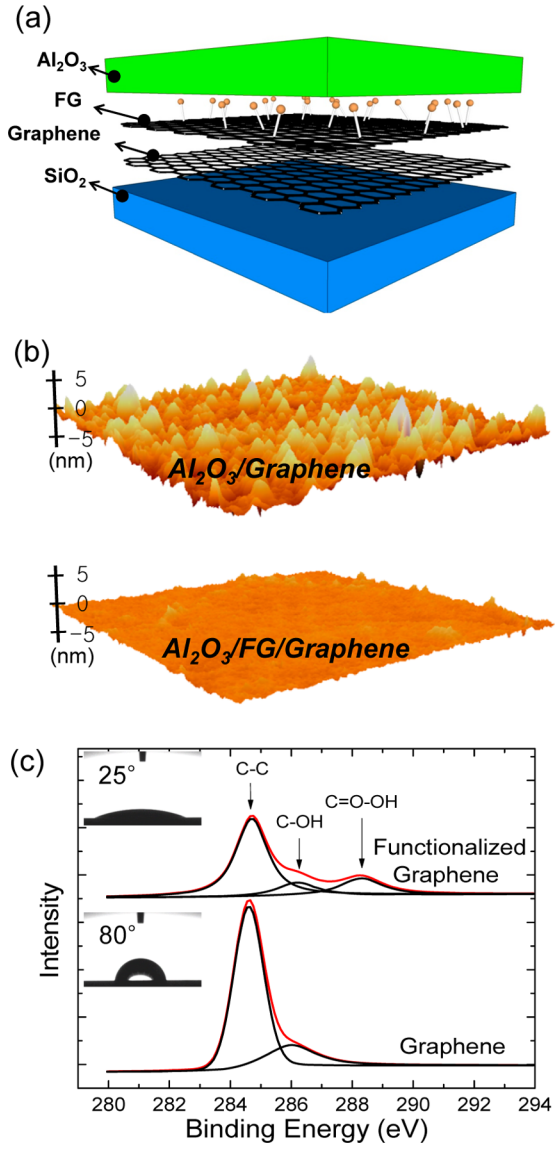

Figure 3. (a) Schematic diagram presenting the FG-seeded Al_2O_3 stack on graphene. (b) Surface morphology of the Al_2O_3 films deposited on graphene (top) and FG/graphene (bottom). The scan size is 1 × 1 μm^2 for all images. The Al_2O_3 film deposited on the FG/graphene exhibited a much smoother surface morphology than that of the Al_2O_3 on bare graphene. (c) C1s XPS spectra of the graphene and FG layer. The inset illustrates the decrease of the graphene contact angle after the functionalization process.

completely covered by the ALD of the Al_2O_3 film, and this was attributed to the intrinsically existing defects in the CVD graphene. However, the ALD Al_2O_3 (20 nm) film remained patchy and discontinuous, thereby resulting in a rough surface (~1 nm) with large pinholes (Figure 3(b)). It is noted that the AFM measurements were performed on the area of 1 × 1 μm^2 and the wrinkle-free graphene region was chosen because CVD-grown and transferred graphene usually has wrinkles on the surface. Figure 3a presents the schematic of the FG-seeded Al_2O_3 film on the graphene. The formation of the FG seed layer was conducted through the wet transfer of the FG layer onto the graphene/SiO_2 substrate. It was observed that the resulting Al_2O_3 film on the FG/graphene exhibited excellent uniformity and low defect density; the root-mean-square (rms) surface roughness of the FG-seeded Al_2O_3 was ~0.3 nm (Figure 3b). In addition, the rms surface roughness of FG-Seeded Al_2O_3 is also lower than previously reported value for Al-seeded Al_2O_3 dielectric.[24] The superb uniformity of the FG-seed Al_2O_3 was attributed to the abundant functional groups contained in the FG seed layer. For the chemical analysis of the FG seed layer, XPS measurements were performed. Figure 3c presents the C1s XPS spectra for both the CVD graphene and FG. The C1s XPS spectra for the CVD graphene had a main C−C bonding peak at 284.7 eV, and there was a small C−OH bonding peak at 286.1 eV.[25] After the functionalization, however, the C−C was decreased and a large number of functional groups including C−OH and C═O−OH were generated. This indicates that the graphene functionalization based on low-density oxygen plasma leads to abundant oxygen-terminated species on the graphene. It was also observed that the contact angle of the CVD graphene decreased after functionalization due to the hydrophilic functional groups (see inset in Figure 3c). It is considered that the abundant functional groups in the FG provide effective nucleation sites, which ultimately facilitate the subsequent ALD on the graphene surface.

To assess the dielectric properties, we fabricated MIG capacitors with Au/Al_2O_3/FG/graphene. Figure 4a presents the schematic cross sectional view and optical image of the fabricated capacitors. For comparison, Au/Al_2O_3/oxidized Al/graphene capacitors were also fabricated in which thin Al metal was deposited using thermal evaporation and oxidized to form a seed layer on the graphene. This technique, which is based on the oxidation of Al metal, has been used widely for the formation of gate dielectrics in graphene field effect transistors.[8] The physical thicknesses for the FG-seeded Al_2O_3 and Al-seeded Al_2O_3 were ~22.3 nm and ~26.2 nm, respectively. Figure 4b presents the capacitance−voltage ($C-V$) characteristics for the Au/Al_2O_3/FG/graphene and Au/Al_2O_3/oxidized Al/graphene capacitors. The V-shape of the CV curve resulted from the existence of the quantum capacitance of graphene.[26] It should be noted that the FG-seeded Al_2O_3 exhibited a capacitance density of ~300 nF/cm^2 at the Dirac voltage. This value was much higher than that of the Al-seeded Al_2O_3 (~210 nF/cm^2). Considering that identical ALD cycles (200 cycles) were used for the Al_2O_3 deposition, the FG seed layer is more desirable for achieving high gate capacitance of ALD dielectrics on graphene. The leakage current and breakdown field distribution of the Al_2O_3 with different seed layers were also measured. The breakdown field is defined as the gate field that produces a gate leakage current density of 5×10^{-5} A/cm^2. As shown in Figure 4c, both the FG-seeded Al_2O_3 and Al-seeded Al_2O_3 exhibited similar breakdown field distributions and the 50% value of the cumulative data was more than 5 MV/cm. In addition, the FG-seeded Al_2O_3 exhibited a low leakage current density of 7 × 10^{-9} A/cm^2 at 3 MV/cm. Figure 4d illustrates the benchmarked data that describes the performance comparison of the ALD dielectrics with different seed layers on graphene. The leakage currents were compared with respect to the equivalent oxide thickness (EOT), which is a common method for evaluating the gate dielectric quality in CMOS device technology. Fallahazad et al. has reported ~400 nF/cm^2 using Ti-seeded Al_2O_3.[10] This can be attributed to much higher dielectric constant (~80) of titanium oxide. However, it is known that TiO_2 is leakier than Al_2O_3 because of small bandgap and large amount of traps.[27] Because they did not report the leakage current of the Ti-seeded Al_2O_3, it is hard to make a direct comparison of their work to our work. It should be noted that the main advantage of our work is to provide

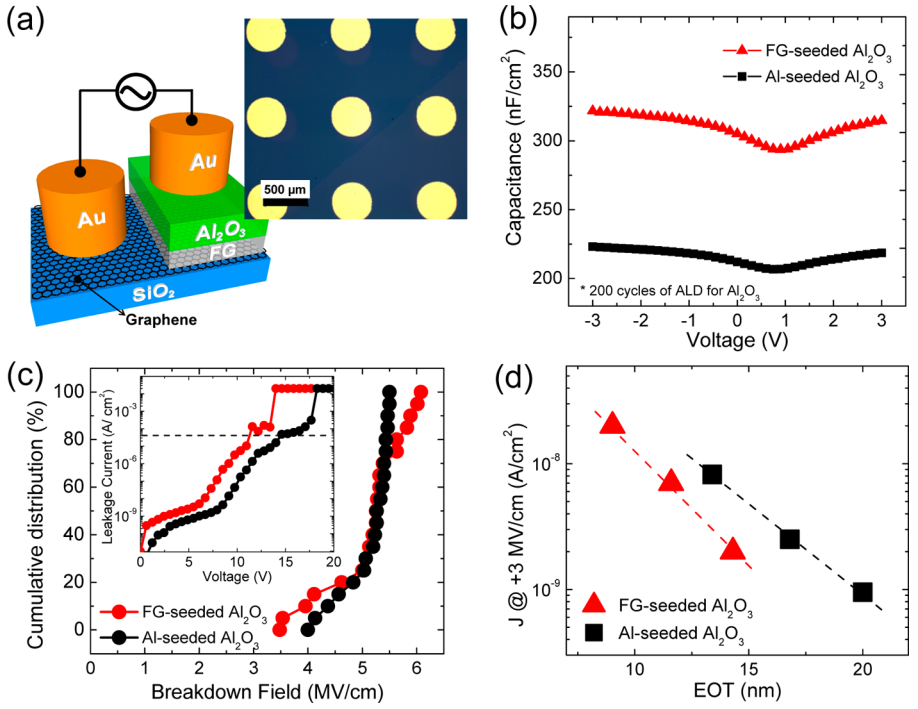

Figure 4. (a) Schematic cross-sectional view of the MIG capacitors with the FG-seeded Al_2O_3 dielectric. Identical ALD conditions (200 cycles of ALD) were used for the A_2O_3 deposition. (b) Capacitance–voltage of the different dielectric stacks (Al_2O_3/FG and Al_2O_3/oxidized Al) on graphene. (c) Cumulative failure of the breakdown field for the Au/Al_2O_3/seed layers/graphene MIG capacitors. (d) Benchmarked data on leakage current densities (at +3 MV/cm^2) versus EOT for dielectrics with different seed layers on graphene.

lower leakage current for the same EOT, which is an important advantage for further scaling of the gate oxide thickness. The FG-seeded Al_2O_3 exhibited a significantly lower leakage current than other dielectrics with polymer[13] or SAM seed layers for the same EOT.[28] Furthermore, the use of the FG seed layer enables a lower EOT compared with that of Al metal seed layers when identical ALD cycles were used in the dielectric deposition; this result is attributed to the use of an ultrathin FG layer. This indicates that the proposed FG seed layer is promising in terms of scaling ALD dielectrics on graphene.

CONCLUSION

It was demonstrated that the FG layer prepared through functionalizing the CVD graphene using a low-density plasma treatment could work as an effective seed layer for the ALD of high-*k* dielectrics on graphene. While identical ALD conditions resulted in patchy and rough dielectric depositions on the graphene, the abundant oxygen species provided through the FG seed layer yielded conformal and pinhole-free Al_2O_3 films on graphene. Because of the beneficial features of the FG seed layer including its ultrathin thickness and abundant nucleation sites, FG-seeded Al_2O_3 exhibits superior scaling capability and low leakage currents for the same equivalent oxide thicknesses.

AUTHOR INFORMATION

Corresponding Author

*E-mail: bjcho@kaist.edu.

Notes

The authors declare no competing financial interest.

ACKNOWLEDGMENTS

This research was supported by the Basic Science Research Program through the National Research Foundation of Korea (NRF) funded by the Ministry of Education, Science and Technology (Grants 2011-0031638, 2010-0029132, and 2012R1A1A1006072).

REFERENCES

(1) Novoselov, K. S.; Geim, A.; Morozov, S.; Jiang, D.; Grigorieva, M. I. K. I. V.; Dubonos, S.; Firsov, A. *Nature* **2005**, *438*, 197.
(2) Zhang, Y.; Tan, Y. W.; Stormer, H. L.; Kim, P. *Nature* **2005**, *438*, 201.
(3) Moon, J.-S. *Carbon Lett.* **2012**, *13*, 1.
(4) Shin, W. C.; Seo, S.; Cho, B. J. *Appl.Phys. Lett.* **2011**, *98*, 153505.
(5) L.Liao, L.; Lin, Y. C.; Bao, M.; Cheng, R.; Bai, J.; Liu, Y.; Qu, Y.; Wang, K. L.; Huang, Y.; Duan, X. *Nature* **2010**, *467*, 305.
(6) Yoon, T.; Shin, W. C.; Kim, T. Y.; Mun, J. H.; Kim, T. S.; Cho, B. J. *Nano Lett.* **2012**, *12*, 1448.
(7) Oh, J. G.; Shin, Y.; Shin, W. C.; Sul, O.; Cho, B. J. *Appl. Phys. Lett.* **2011**, *99*, 193503.
(8) Garces, N. Y.; Wheeler, V. D.; Gaskill, D. K. *J. Vac. Sci. Technol., B* **2012**, *30*, 030801.
(9) Xuan, Y.; Wu, Y.; Shen, T.; Qi, M.; Capano, M. A.; Cooper, J. A.; Ye, P. *Appl. Phys. Lett.* **2008**, *92*, 013101.
(10) Fallahazad, B.; Lee, K.; Lian, G.; Kim, S.; Corbet, C.; Ferrer, D.; Colombo, L.; Tutuc, E. *Appl. Phys.Lett.* **2012**, *100*, 093112.
(11) Robinson, J. A.; LaBella, M., III; Trumbull, K. A.; Weng, X.; Cavelero, R.; Daniels, T.; Hughes, Z.; Hollander, M.; Fanton, M.; Snyder, D. *ACS Nano* **2010**, *4*, 2667.
(12) Shen, T.; Gu, J.; Xu, M.; Wu, Y.; Bolen, M.; Capano, M.; Engel, L.; Ye, P. *Appl. Phys. Lett.* **2009**, *95*, 172105.
(13) Shin, W. C.; Kim, T. Y.; Sul, O.; Cho, B. J. *Appl.Phys. Lett.* **2012**, *101*, 033507.
(14) Farmer, D. B.; Chiu, H.-Y.; Lin, Y.-M.; Jenkins, K. A.; Xia, F.; Avouris, P. *Nano Lett.* **2009**, *9*, 4474.
(15) Meric, I.; Dean, C. R.; Young, A. F.; Baklitskaya, N.; Tremblay, N. J.; Nuckolls, C.; Kim, P.; Shepard, K. L. *Nano Lett.* **2011**, *11*, 1093.
(16) Nayfeh, O. M.; Marr, T.; Dubey, M. *IEEE Electron Device Lett.* **2011**, *32*, 473.

(17) Lee, B.; Mordi, G.; Kim, M.; Chabal, Y.; Vogel, E.; Wallace, R.; Cho, K.; Colombo, L.; Kim, J. *Appl.Phys. Lett.* **2010**, *97*, 043107.
(18) Kim, D. C.; Jeon, D.-Y.; Chung, H.-J.; Woo, Y.; Shin, J. K.; Seo, S. *Nanotechnology* **2009**, *20*, 375703.
(19) Lu, X.; Huang, H.; Nemchuk, N.; Ruoff, R. S. *Appl.Phys. Lett.* **1999**, *75*, 193.
(20) Shin, W. C.; Moon, H.; Yoo, S.; Li, Y.; Cho, B. J. *IEEE Electron Dev. Lett.* **2010**, *31*, 1308.
(21) Yang, D.; Velamakanni, A.; Bozoklu, G.; Park, S.; Stoller, M.; Piner, R. D.; Stankovich, S.; Jung, I.; Field, D. A.; Ventrice, C. A., Jr *Carbon* **2009**, *47*, 145.
(22) Kudin, K. N.; Ozbas, B.; Schniepp, H. C.; Prud'Homme, R. K.; Aksay, I. A.; Car, R. *Nano Lett.* **2008**, *8*, 36.
(23) Wang, X.; Tabakman, S. M.; Dai, H. *J. Am. Chem. Soc.* **2008**, *130*, 8152.
(24) Hollander, M. J.; Labella, M.; Hughes, Z. R.; Zhu, M.; Trumbull, K. A.; Cavalero, R.; Snyder, D. W.; Wang, X.; Hwang, E.; Datta, S.; Robinson, J. A. *Nano Lett.* **2011**, *11*, 3601.
(25) Hong, S. K.; Song, S. M.; Sul, O.; Cho, B. J. *J. Electrochem. Soc.* **2012**, *159*, K107.
(26) Giannazzo, F.; Sonde, S.; Raineri, V.; Rimini, E. *Nano Lett.* **2008**, *9*, 23.
(27) Fulton, C. C.; Lucovsky, G.; Nemanich, R. J. *J. Vac. Sci. Technol., B* **2002**, *20*, 1726.
(28) Alaboson, J. M.; Wang, Q. H.; Emery, J. D.; Lipson, A. L.; Bedzyk, M. J.; Elam, J. W.; Pellin, M. J.; Hersam, M. C. *ACS Nano* **2011**, *5*, 5223.